Computing the Anharmonic Vibrational Spectrum of UF6 in 15 Dimensions with an Optimized Basis Set and Rectangular Collocation

ARTICLE *in* THE JOURNAL OF PHYSICAL CHEMISTRY A · AUGUST 2015

Impact Factor: 2.69 · DOI: 10.1021/acs.jpca.5b07627 · Source: PubMed

THE JOURNAL OF PHYSICAL CHEMISTRY A

Article

pubs.acs.org/JPCA

Computing the Anharmonic Vibrational Spectrum of UF_6 in 15 Dimensions with an Optimized Basis Set and Rectangular Collocation

Published as part of The Journal of Physical Chemistry A virtual special issue "Spectroscopy and Dynamics of Medium-Sized Molecules and Clusters: Theory, Experiment, and Applications".

Sergei Manzhos,*[,†] Tucker Carrington,[‡] Laura Laverdure,[‡] and Nicholas Mosey[‡]

[†]Department of Mechanical Engineering, National University of Singapore, Block EA #07-08, 9 Engineering Drive 1, Singapore 117576

[‡]Department of Chemistry, Queen's University, Chernoff Hall, 90 Bader Lane, Kingston, ON, Canada K7L 3N6

ABSTRACT: The anharmonic vibrational spectrum of UF_6 is computed in full dimensionality directly from ab initio data, i.e., bypassing the construction of a potential energy surface (PES). The vibrational Schrödinger equation is solved by fitting parameters of an adaptable basis using a modified version of the rectangular collocation algorithm of Manzhos and Carrington (*J. Chem. Phys.* **2013**, *139*, 051101). The basis functions are products of parametrized Hermite polynomials that impose approximate nodal structure. The Schrödinger equation is solved in normal coordinates. The results show that anharmonicity and coupling do noticeably affect the vibrational transitions, shifting them by several cm^{-1}. Although UF_6 has 15 coordinates, we compute hundreds of levels with fewer than 1000 basis functions and about 50 000 ab initio points. It is the efficiency of the basis that makes it possible to forego a PES.

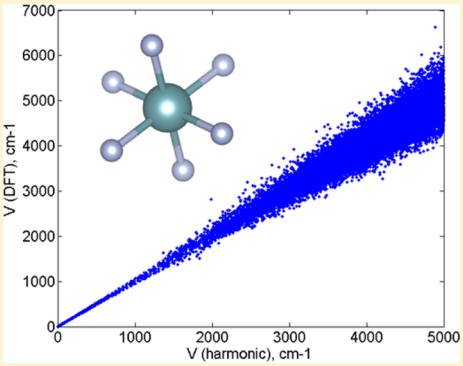

INTRODUCTION

The vibrational spectrum of UF_6 is important for the detection[1] of UF_6 isotopologues as well as for possible use in laser-driven UF_6 enrichment.[2,3] Laser-driven enrichment may be more economical because a single pass can be sufficient to enrich $^{235}UF_6$ from its natural abundance of around 0.7% to the abundance of 3−5% required for use in nuclear fuels.[4] This is in contrast to tedious multistage diffusion-based enrichment techniques, which have dominated nuclear technology for decades. Owing to the poor efficiency of diffusion-based methods, the enrichment step can be responsible for up to 10% of the cost of generating electricity.[5] Schemes based on excitation of both pure U (e.g., atomic vapor laser isotope separation (AVLIS[6,7]) and UF_6 molecules (e.g., MLIS/SILEX[7]) have been proposed.[3] UF_6 is part of the current fuel cycle, and it is advantageous to base any new enrichment scheme on UF_6. It is easier to use vibrational excitation where the required relative resolution is on the order of 10^{-3}. This is in contrast with, for example, the AVLIS technique, which uses the hyperfine structure of the uranium atom, specifically, the absorption peak at 502.74 nm of ^{238}U, which shifts to 502.73 nm in ^{235}U, requiring relative resolution on the order of 10^{-5}. Specifically, the strongest IR active isotopologue-sensitive mode of UF_6 at 626 cm^{-1} differs by about 0.6 cm^{-1} in $^{235}UF_6$ and $^{238}UF_6$.[8] Usually, the assignment of spectral features of UF_6 is done using a harmonic approximation.[2,9,10] Although the harmonic approximation makes it possible to assign major features, the effects of anharmonicity and coupling on the vibrational spectrum could be important enough to affect isotopologue-selective excitation. Moreover, even harmonic transition energies have been reported in a wide range in computational literature. For example, values in the range of 576−636 cm^{-1} were reported for the mode most sensitive to isotope replacement.[9,10] The effects of anharmonicity and coupling among all modes of UF_6 remain unquantified.

Computing the anharmonic spectrum of UF_6 is difficult because it has 15 vibrational coordinates. Approximate methods such as low-order perturbation theory[11] and vibrational self-consistent field (VSCF)[12,13] might be used but they are computationally costly and intrinsically inaccurate. Perturbation theory is usually implemented with a Taylor series representation of the potential energy surface (PES). For a molecule with 7 atoms, even if many of the terms are neglected, the number of quartic terms is huge and summing contributions from them all would be expensive. VSCF is often implemented by computing the potential at the points of many low-dimensional grids. The number of such grids is large for a molecule with 7 atoms. In addition, the VSCF approximation makes it impossible to account for some coupling in the kinetic energy operator (KEO).

Rather than using a method that is intrinsically approximate, we opt for a collocation approach. When a standard product basis is used, both the basis size and the quadrature or collocation grid, required for potential matrix elements are enormous.[14−16] When the vibrational Schrödinger equation is solved,

$$\hat{H}\psi(\mathbf{r}) = (\hat{T} + V(\mathbf{r}))\psi(\mathbf{r}) = E\psi(\mathbf{r}) \quad (1)$$

Received: August 6, 2015
Revised: August 21, 2015
Published: August 21, 2015

DOI: 10.1021/acs.jpca.5b07627
J. Phys. Chem. A 2015, 119, 9557−9567

where $\hat{T}$ is the KEO, $V(\mathbf{r})$ is the potential energy surface, E is the energy, $\psi(\mathbf{r})$ is the wave function, and $\mathbf{r}$ is a vector in configuration space, one typically expands the wave function in a basis:

$$\psi(\mathbf{r}) = \sum_{i=1}^{N} c_i \phi_i(\mathbf{r}) \tag{2}$$

where $\phi_i(\mathbf{r})$ is a product of functions of one coordinate. The coefficients can be determined by using collocation by substituting expansion (2) into the Schrödinger equation (1) and demanding that it be satisfied at a set of points $\mathbf{r}_j$, $j = 1, ..., M$:

$$\sum_{i=1}^{N} c_i \hat{H}\phi_i(\mathbf{r}_j) = E \sum_{i=1}^{N} c_i \phi_i(\mathbf{r}_j) \tag{3}$$

or, in matrix form,

$$\mathbf{Hc} = E\mathbf{\Phi c} \tag{4}$$

where $H_{ji} = H\hat{\phi}_i(\mathbf{r}_j)$ and $\Phi_{ji} = \phi_i(\mathbf{r}_j)$. This is a rectangular matrix equation for a vector of coefficients $\mathbf{c}$. When $N = M$, it is a conventional (square) collocation eigenvalue problem.[17] Such a collocation method has been used for low-dimensional problems.[18,19] By replacing the basis expansion with a Smolyak interpolant, one can also solve higher dimensional problems.[20] Both the size of the basis and the size of the grid become prohibitive as the dimensionality of the problem increases.

The variational approach[21] is another means of determining the coefficients in eq 3. One multiplies on the left by a basis function and integrates to obtain

$$\tilde{\mathbf{H}}\mathbf{c} = E\mathbf{Sc} \tag{5}$$

Here $\tilde{H}_{ij} = \langle \phi_i(\mathbf{r}) | \hat{H} | \phi_j(\mathbf{r}) \rangle$ and $S_{ij} = \langle \phi_i(\mathbf{r}) | \phi_j(\mathbf{r}) \rangle$. Insofar as the integrals are computed numerically, this is equivalent to starting with (rectangular) eq 4, where $\mathbf{r}_j$ are points on the quadrature grid, and multiplying on the left with $\mathbf{\Phi}^{\mathrm{T}}$ to make a square eigenvalue problem. *That is, from the rectangular collocation equation (4) one can derive both the conventional (square) collocation method and the variational method.* The accuracy of E and $\mathbf{c}$ in (5), regardless of whether $N = M$ or $M > N$, depends on how complete the basis is and on the choice of the quadrature points and weights. The better the basis is, the less important is the quadrature error.[22] When basis functions are products of functions of a single coordinate, very large N and M are typically required. By using basis functions that are eigenfunctions of reduced-dimension Hamiltonians or localized in phase space,[23−25] one can drastically reduce the size of the basis.[26−30] In this paper we use parametrized adaptable basis functions.

We have recently developed a method that adapts the basis functions to the potential by tuning basis parameters.[31,32] It uses the rectangular collocation equation (4), which is a so-called rectangular matrix pencil and in general is only satisfied approximately, e.g., in the least-squares sense.[33] The shape of the basis and E are tuned to minimize the norm of the difference of the LHS and RHS of eq 4. This is achieved by parametrizing $\phi_i(\mathbf{r})$, i.e., using $\phi_i(\mathbf{r}|\boldsymbol{\lambda})$, where $\boldsymbol{\lambda}$ are the parameters. The method is described in more detail below. The tuning process requires $M > N$, although at fixed $\boldsymbol{\lambda}$, there is no advantage of using the rectangular version of eq 4 over square collocation.[34] The method allows one to compute spectra without neglecting anharmonicity and coupling, as does also the variational method. An exact KEO, in any coordinates, can be used, and the PES may have a complex shape. Because the basis is flexible, N can be small, and M can be small enough that all $V_j \equiv V(\mathbf{r}_j)$ can be computed *ab initio*, thereby obviating the need to construct a continuous PES. This is a significant advantage, as fitting an analytical PES for systems with more than about six degrees of freedom is a difficult task and necessarily introduces error.[35−37] When the number of quadrature or collocation points required to compute the spectrum is large, it is nevertheless better to fit or interpolate than to calculate the potential at all of the points. Owing to the fact that wave functions have more structure than potentials, this is often the case. However, the number of required points is often inflated by choosing a poor basis. To date, calculations done with the tunable basis rectangular collocation approach had two limitations: (1) the accuracy was never better than about 1 cm^{-1} (which is worse than that which is achieved with variational approaches), and (2) only a few levels were computed. However, the method is clearly well suited for problems for which the required accuracy of the calculation is of the order of 1 cm^{-1} (for example, where experimental data are not more accurate), where only several vibrational levels are of interest, and where there is no available PES. Many practically important systems, e.g., most interfacial systems, satisfy all or some of these conditions. For example, the accuracy of spectra at surfaces is usually limited to 1−4 cm^{-1},[38−40] only the fundamental transitions are usually of interest, and for the overwhelming majority of interfaces studied in laboratories, PESs will never be built. These conditions are also satisfied for certain single-molecule systems, of which UF_6 is an example: the accuracy of most lines of experimental IR and Raman spectra is not better than 1 cm^{-1},[1,8] and a fully coupled *ab initio* based PES for UF_6 is not available. This has to do, in particular, with the sheer dimensionality of the configuration space −15. The rectangular collocation method has been previously used in up to 7 dimensions.[32]

The reported vibrational spectrum of UF_6 is assigned for up to 3 quanta of excitation in some of the vibrational modes.[8] To compare with experiment, it is therefore necessary to compute hundreds of vibrational levels. This is difficult with the rectangular collocation approach of ref 32. Previously, only fundamentals or lowest excitations were computed: 5 levels of H_2O,[41] molecular fundamentals of H_2O on Pt[42] and of formate on AuPt,[43] and selected fundamentals of acetic acid on TiO_2.[31] In the rectangular collocation calculations of this paper, it is also necessary to deal with the fact that the fundamentals of UF_6 span a large range: from 136 to 678 cm^{-1} (with the *ab initio* method used here). Because the range and dimensionality are large, the range includes many combination bands and the density of states is high. This makes fitting difficult because the algorithm is prone to jump between nearby states. We therefore present a modification of the method that effectively deals with these issues. Specifically, we compute 816 vibrational levels, sufficient for the assignment of the experimental spectrum. In this paper, we address both of the limitations referred to above. We show that in some cases accuracy can be better than 1 cm^{-1} (cf. results of the calculation on the harmonic PES below) and we introduce new ideas that make it possible to calculate many levels.

METHODS

Electronic structure calculations were performed using density functional theory (DFT)[44,45] with the hybrid PBE0 functional.[46−48] A 60-electron relativistic effective core potential (ECP) was used to treat the core electrons of uranium.[49−51] The valence electrons of uranium were treated with the associated SDD basis set,[49−51] and a TZVP basis set[52] was applied to fluorine. All calculations were performed with the Gaussian 09 software package.[53] Symmetry was imposed during the

DOI: 10.1021/acs.jpca.5b07627
J. Phys. Chem. A 2015, 119, 9557−9567

Table 1. Harmonic Vibrational Transitions of $^{235}UF_6$ and Isotopic Splittings, in cm^{-1} [a]

		experiment		DFT harmonic		collocation, fit(eig)	
symmetry	type of mode	transition	235−238	transition	235−238	transition	235−238
f_{2u}	deg deform, ν_6	143 ± 2	0	136.21	0	136.24(08)	−0.08(08)
						136.24(13)	−0.08(08)
						136.24(25)	−0.08(08)
f_{1u}	deg deform, ν_4	186.2 ± 0.5	0.16 ± 0.1	181.28	0.20	181.32(15)	0.12(21)
						181.32(17)	0.12(21)
						181.32(32)	0.12(21)
f_{2g}	deg deform, ν_5	200.4 ± 1	0	199.02	0	199.06(198.92)	−0.05(08)
						199.06(03)	−0.05(08)
						199.06(06)	−0.05(07)
e_g	deg str, ν_2	534.1 ± 0.5	0	538.94	0	538.98(96)	−0.07(08)
						538.98(98)	−0.07(08)
f_{1u}	deg str, ν_3	625.5 ± 0.5	0.65 ± 0.1	628.05	0.61	628.09(04)	0.52(81)
						628.09(05)	0.52(81)
						628.09(09)	0.52(81)
a_{1g}	sym str, ν_1	667.1 ± 0.2	0	677.94	0	677.98(98)	−0.05(08)

[a]The experimental data are from ref 8. In the "collocation" columns the first number is the result obtained by simultaneously fitting the basis and the energy, eqs 10 and 11, and the number in brackets is the fractional part of the result obtained when the fitted basis is used with the squared collocation eigenproblem, eq 12. In all rows accept the third the integer parts are the same with both methods.

optimization and normal mode calculations. The geometry and vibrational frequencies computed with this setup agree well with available experimental data and previous calculations (Table 1),[8,10,54−58] and the cost is reasonable. Several other approaches were tried, including ECPs with different core sizes, larger basis sets, or all-electron calculations with the ZORA treatment of the relativistic effects.[59] Harmonic transitions calculated with these different approaches can differ from those obtained with our chosen setup by about 10 cm^{-1}. Calculations at 3500 randomly selected structures showed that using the QZVP basis set[60] used to treat fluorine changed the energies calculated relative to that of the optimized structure of UF_6 by ∼13 cm^{-1} on average when compared with the energies obtained with the computational setup described above. However, the use of a larger basis set on F increased the computational demands of the calculations considerably.

The potential energy surface was sampled with pseudorandom points (Sobol sequence[61]) chosen within ranges of the normal mode coordinates computed by DFT. The maximum normal mode displacements were chosen as[62]

$$Q_{d,\max} = \frac{6}{\sqrt{2\pi\omega_d}} \qquad d = 1, ..., 15 \tag{6}$$

where ω_d are the normal-mode frequencies (in a.u.) and points were accepted if $V_{\mathrm{harm}}(\mathbf{Q}) < V_{\max} = 5000\ cm^{-1}$, where V_{harm} is a harmonic potential built from normal-mode frequencies computed with DFT. Q_d is a dimensionless normal coordinate. Points along normal mode slices (where only one of the Q_d is nonzero) up to $Q_{d,\max}$ were added to the data set (1500 points with 100 points per slice). Given the extremely low sampling density, additional points were added near the extrema of the basis functions of eq 8 (but with $\alpha_d = 0$, $\gamma_d = 0$, $\chi_d = 0$) (about 5000 points) to make sure there are collocation points where the basis functions have significant amplitude. This was done to make coefficients of those basis functionals well-determined. A total of 50 000 points were computed. If the points were on a multidimensional rectangular grid with the same number of points for each coordinate, then there would be only 2.06 points per degree of freedom (DOF). Of course, such a direct product grid is completely impractical. The simplest possible Smolyak grid with 7 basis functions per coordinate has 54 264 functions.[63]

The vibrational Schrödinger equation was solved with a modified version of the rectangular collocation method of Manzhos and Carrington, in which the wave function is expanded in a parametrized basis:

$$\psi(\mathbf{Q}) = \sum_{i=1}^{N} c_i \phi_i(\mathbf{Q}|\boldsymbol{\lambda}) \tag{7}$$

where $\mathbf{Q}$ is a vector of normal mode coordinates, $\boldsymbol{\lambda}$ is a vector of parameters, and N is the basis size. We use basis functions that are parametrized harmonic wave functions:

$$\phi_i(\mathbf{Q}) = \prod_{d=1}^{D} \frac{e^{-1/2\tilde{Q}_d^2}}{\sqrt{2^n n!\sqrt{\pi}}} H_{n(i,d)}(\tilde{Q}_d^2) \tag{8}$$

where $\tilde{Q}_d = \alpha_d + \beta_d Q_d + \gamma_d Q_d^2 + \chi_d Q_d^3$, i.e., $\boldsymbol{\lambda}_d = (\alpha_d, \beta_d, \gamma_d, \chi_d)$. $H_{n(i,d)}$ are Hermite polynomials of order n. Note that $\boldsymbol{\lambda}$ depends on d (i.e., on the normal mode Q) but not on n (i.e., all basis function components depending on the same Q have the same parameters). We have previously shown that this significantly reduces the cost of fitting without significantly affecting the accuracy, for systems with moderate anharmonicity, as is the case here.[62] The orders $n(i,d)$ satisfy $n(i,d) \le n_{\max}$, $\Sigma_{d=1}^{D} n(i,d) \le n_{\max}$.[14,64] We use $n_{\max} = 3$ and therefore $N = 816$. $n_{\max} = 3$ corresponds to the maximum number of excitations in the assigned spectrum.[8] The method we use to solve the Schrödinger equation is not limited to a particular type of basis, but the Hermite basis imposes an appropriate nodal structure on the wave function and therefore allows one to use many fewer basis functions and potential points than would be required, for example with a parametrized Gaussian basis, which can and has been successfully used for problems of smaller dimensionality.[41,42,62]

We use an uncoupled kinetic energy operator (KEO), $\hat{T} = (-1/2)\Sigma_{d=1}^{D}(\partial^2/\partial Q_d^2)$, and further approximate its action of on the basis functions as

$$\hat{T}\phi_i(\mathbf{Q}) = -\frac{1}{2}\sum_{d=1}^{D}\frac{\partial^2\phi_i}{\partial Q_d^2} \approx -\frac{1}{2}\phi_i(\mathbf{Q})\sum_{d=1}^{D}(\tilde{Q}_d^2 - 2n(i,d) - 1)\left(\frac{\partial\tilde{Q}_d}{\partial Q_d}\right)^2 \tag{9}$$

DOI: 10.1021/acs.jpca.5b07627
J. Phys. Chem. A 2015, 119, 9557−9567

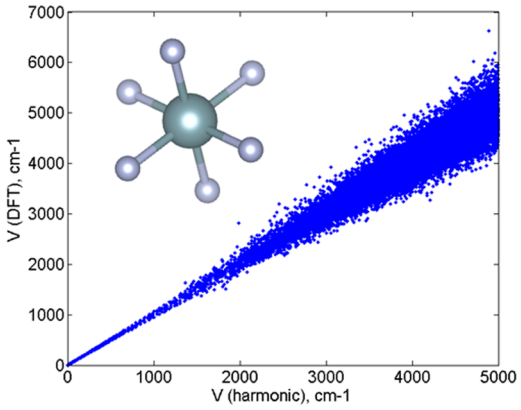

Figure 1. DFT energies vs harmonic potential energies. The UF_6 molecule is shown in the inset.

In eq 9, we have neglected the term proportional to $\partial^2\tilde{Q}_d/\partial Q_d^2$. Although the method of rectangular collocation can be used with any coordinates and KEOs (e.g., an exact KEO was used in ref 41), we use this approximate KEO for numerical efficiency. The approximation to the second derivative operator that we use here changes the ZPE by a few cm^{-1} but changes the transition wavenumbers by less than 0.1 cm^{-1}, as was confirmed in refs 31 and 43 and is also confirmed here in the harmonic test (vide infra).

The rectangular collocation equation (4) was solved for a small number of vibrational levels with the basis (8) and KEO (9):

$$(\mathbf{H} - E_k\mathbf{\Phi})\mathbf{c_k} = \mathbf{0} \tag{10}$$

where k indexes vibrational levels. The basis parameters and energy were fitted to minimize

$$R = \frac{1}{L}\sum_{k=1}^{L}\frac{\|((\mathbf{H} - E_k\mathbf{\Phi})\mathbf{c_k})\|}{E_k\|\mathbf{\Phi c_k}\|} \tag{11}$$

where L is the number of levels. The fit was done for the ZPE and fundamentals with only 16 basis functions. Because only 16 basis functions are used, the fit imposes the correct nodal structure on the basis functions and there is no jumping between states as the parameters are varied. If a larger number of basis functions is used, then, due to the high vibrational density of states, the fit hops between neighboring levels. The fit is done in Matlab[65] using the *fmincon* function with the interior-point algorithm, and a 16-level fit takes of the order of an hour on a multicore workstation. Parameters were constrained to remain within physically meaningful ranges during the fit. With the *ab initio* data used here, the order of magnitude of the parameters is (depending on the mode) $\alpha \sim -0.01 \ldots 0.01$, $\beta \sim 0.02 \ldots 0.06$, $\gamma \sim -0.003 \ldots 0.004$, $\chi \sim -0.002 \ldots 0.004$. Note that only β is nonzero in the harmonic case. After the parameters were fitted, $N = 816$ levels were computed from the squared collocation eigenvalue equation

$$\mathbf{\Phi}^T\mathbf{H}\mathbf{c} = E\mathbf{\Phi}^T\mathbf{\Phi}\mathbf{c} \tag{12}$$

This takes under a minute on a typical workstation.

The spectra of both $^{235}UF_6$ and $^{238}UF_6$ were computed from the same *ab initio* energies by using the coordinate conversion

$$Q^{238} = (L^{238})^T(M^{238})^{1/2}(M^{235})^{-1/2}L^{235}Q^{235} \tag{13}$$

where $Q^{235/238}$ are normal mode coordinates of the two isotopologues, $L^{235/238}$ are their normal mode vectors (obtained by diagonalizing the raw Hessian matrix output by Gaussian 09 using the appropriate $M^{235/238}$), and $M^{235/238}$ is a diagonal matrix containing the atomic masses. Equation 13 is correct close to the equilibrium geometry. Replacing ^{235}U with ^{238}U changes neither the position of the center of mass nor the orientation of the molecule-fixed axes at the equilibrium geometry. Contrary to statements in the literature,[66] after Q^{238} is obtained from Q^{235}, there is no need to work with a potential that depends on vibrational and rotational Q^{238} normal coordinates.

We compute only the spectrum of vibrational levels; calculation of intensities is not implemented.

RESULTS

Table 1 lists the *ab initio* harmonic frequencies of UF_6, their assignments, and the isotopologue splittings. The equilibrium UF bond length, 1.989 Å, the normal-mode frequencies, and the splittings between $^{235}UF_6$ and $^{238}UF_6$ agree well with available

Table 2. Fundamental Transitions of $^{238}UF6$ (from the Harmonic and Anharmonic Calculations)[a]

		235−238		
harm	anharm	harm	anharm	character
135.82	142.26	−0.01	0.02	**100** 000 000 00 000 0
135.84	146.61	−0.01	0.05	**001** 000 000 00 000 0
135.88	148.88	−0.01	0.04	**010** 000 000 00 000 0
180.68	191.96	0.19	0.28	000 **010** 000 00 000 0
180.71	192.59	0.18	0.29	000 **100** 000 00 000 0
180.77	195.76	0.18	0.26	000 **001** 000 00 000 0
198.64	210.41	−0.01	−0.03	000 000 **100** 00 000 0/1 000 000 **001** 00 000 0/0.4 000 000 **010** 00 000 0/0.3
198.69	218.46	−0.02	0.48	000 000 **010** 00 000 0/1 000 000 **001** 00 000 0/0.6
198.73	222.45	−0.01	−0.30	000 000 **100** 00 000 0/0.6 000 000 **001** 00 000 0/1 000 000 **010** 00 000 0/0.6
538.61	527.09	−0.01	−0.44	000 000 000 **10** 000 0/1 000 000 000 **01** 000 0/0.06
538.63	534.32	−0.01	−0.96	000 000 000 **01** 000 0/1 001 000 011 **00** 000 0/0.8 001 000 020 **00** 000 0/0.3
627.09	630.38	0.59	0.63	000 000 000 00 **001** 0/1
627.11	632.66	0.60	0.58	000 000 000 00 **010** 0/1 000 000 000 00 **001** 0/0.23
627.12	633.41	0.60	0.57	000 000 000 00 **100** 0/1 000 000 000 00 **001** 0/0.24 000 000 000 00 **010** 0/0.11
677.61	685.68	−0.01	0.03	000 000 000 00 000 **1**/1

[a]See Table 1 for experimental transitions. Leading basis functions (with relative amplitudes above 0.1) used to assign the transitions and their relative amplitudes (after "/") are also given. The basis function character is given by a list of $n(i,d)$, $d = 1, \ldots, 15$. In bold are highlighted normal modes where excitations (non-zero n values) are expected on the basis of the experimental assignments.

DOI: 10.1021/acs.jpca.5b07627
J. Phys. Chem. A 2015, 119, 9557−9567

Table 3. Vibrational Transitions of $^{238}UF_6$ (from the Harmonic and Anharmonic Calculations) Assigned to the Experimental (exp) Raman and IR Spectra[5,a]

exp	assignment	harm	anharm	character
				Raman
1331.9 ± 1	$2\nu_1$	1355.2	1348.0	000 000 000 00 000 **2**/1 010 000 000 10 000 **1**/0.11
1197 ± 2	$\nu_1 + \nu_2$	1216.2	1209.1	000 000 000 **10** 000 **1**/1 010 000 000 **01** 000 **1**/0.17
			1210.2	000 000 000 **01** 000 **1**/1 000 000 000 **10** 000 **1**/0.3
1066.3 ± 1	$2\nu_2$	1077.2	1067.7	000 000 000 **02** 000 0/0.9 000 000 200 **00** 000 1/1 000 000 002 **00** 000 1/0.67
867 ± 2	$\nu_1 + \nu_5$	876.3	871.2	000 000 **100** 00 000 **1**/1 010 000 **010** 10 000 **1**/0.98 010 000 **001** 10 000 **1**/0.3
			871.9	000 000 **001** 00 000 **1**/1 000 000 **100** 00 000 **1**/0.18 000 000 **010** 00 000 **1**/0.17
			874.8	000 000 **010** 00 000 **1**/1 100 000 **010** 10 000 **0**/0.23 000 000 **001** 00 000 **1**/0.12
811.2 ± 0.5	$\nu_3 + \nu_4$	807.8	804.4	000 **001** 000 00 **001** 0/1 807.5 000 **001** 000 00 **010** 0/1
			809.7	000 **001** 000 00 **100** 0/1 802.2 000 **010** 000 00 **001** 0/1
			805.3	000 **010** 000 00 **010** 0/1 802.1 000 **010** 000 00 **001** 0/1
			809.7	000 **001** 000 00 **100** 0/1 804.9 000 **100** 000 00 **010** 0/1
			804.8	000 **100** 000 00 **100** 0/1
765 ± 3	$\nu_3 + \nu_6$	763.0	756.3	**001** 000 000 00 **001** 0/1 759.2 **001** 000 000 00 **100** 0/1
			760.1	**001** 000 000 00 **001** 0/1 761.7 **100** 000 000 00 **001** 0/1
			762.1	**100** 000 000 00 **010** 0/1 762.5 **010** 000 000 00 **001** 0/1
			764.3	**010** 000 000 00 **100** 0/1 765.2 **100** 000 000 00 **100** 0/1
			765.6	**010** 000 000 00 **010** 0/1
399 ± 2	$2\nu_5$	397.4	391.0	000 000 **200** 00 000 0/1 000 000 **110** 00 000 0/0.5 000 000 **002** 00 000 0/0.3
			396.0	000 000 **020** 00 000 0/1 000 000 **110** 00 000 0/0.66 000 000 **101** 00 000 0/0.46
375 ± 2	$2\nu_4$	361.4	359.1	000 **002** 000 00 000 0/1 000 **020** 000 00 000 0/0.2
			355.5	000 **020** 000 00 000 0/1 000 **200** 000 00 000 0/0.17 000 **002** 000 00 000 0/0.12
			356.8	000 **200** 000 00 000 0/1 000 **020** 000 00 000 0/0.55 000 **002** 000 00 000 0/0.14
281 ± 2	$2\nu_6$	271.7	263.1	**002** 000 000 00 000 0/1 **200** 000 000 00 000 0/0.21 **000** 000 001 00 000 0/0.14
			271.0	**020** 000 000 00 000 0/1 **002** 000 000 00 000 0/0.5
				IR
1955 ± 3	$2\nu_1 + \nu_3$	1982.3	1981.3	000 000 000 00 **001** **2**/1
			1982.9	000 000 000 00 **100** **2**/1
			1983.6	000 000 000 00 **010** **2**/1
1870.5 ± 2	$3\nu_3$	1881.2	1883.2	000 000 000 00 **003** 0/1 000 000 000 00 **111** 0/0.76 000 000 000 00 **021** 0/0.75
			1888.9	000 000 000 00 **300** 0/1 000 000 000 00 **102** 0/0.64 000 000 000 00 **111** 0/0.18
1821 ± 2	$\nu_1 + \nu_2 + \nu_3$	1843.3	1840.4	000 000 000 **01** **001** **1**/1 000 000 000 **10** **001** **1**/0.58
			1842.9	000 000 000 **01** **010** **1**/1 000 000 000 **10** **010** **1**/ 0.16
			1846.3	000 000 000 **01** **100** **1**/1 000 000 000 **10** **100** **1**/0.11
			1841.3	000 000 000 **10** **001** **1**/1 000 000 000 **10** **001** **1**/0.17 000 000 000 **10** **100** **1**/0.16
			1843.1	000 000 000 **10** **010** **1**/1 000 000 000 **01** **010** **1**/0.35
			1841.7	000 000 000 **10** **100** **1**/1 000 000 000 **10** **001** **1**/0.18
1687.5 ± 2	$2\nu_2 + \nu_3$	1704.4	1693.5	000 000 000 **02** **001** 0/1 000 000 000 **20** **001** 0/0.51
			1694.5	000 000 000 **20** **010** 0/1 000 000 000 **02** **010** 0/0.83
			1701.2	000 000 000 **02** **100** 0/1 000 000 000 **11** **001** 0/0.15
			1697.6	000 000 000 **20** **001** 0/1 000 000 000 **11** **001** 0/0.68 000 000 000 **20** **010** 0/0.65
			1695.3	000 000 000 **20** **100** 0/1 000 000 000 **02** **100** 0/0.77
1519 ± 2	$2\nu_1 + \nu_4$	1535.9	1532.1	000 **001** 000 00 000 **2**/1
			1529.4	000 **010** 000 00 000 **2**/1 000 **100** 000 00 000 **2**/0.37
			1529.5	000 **100** 000 00 000 **2**/1 000 **010** 000 00 000 **2**/0.35
1486.5 ± 2	$\nu_1 + \nu_3 + \nu_5$	1503.4	1503.8	000 000 **001** 00 **001** **1**/1 000 000 **010** 00 **001** **1**/0.21
			1505.1	000 000 **001** 00 **010** **1**/1 000 000 **100** 00 **010** **1**/0.18
			1505.7	000 000 **001** 00 **100** **1**/1 000 000 **100** 00 **100** **1**/0.20
			1506.9	000 000 **010** 00 **001** **1**/1 000 000 **010** 00 **010** **1**/0.34 000 000 **001** 00 **001** **1**/0.18
			1507.9	000 000 **010** 00 **100** **1**/1 000 000 **001** 00 **100** **1**/0.14
			1501.6	000 000 **100** 00 **001** **1**/1
			1503.1	000 000 **100** 00 **010** **1**/1 000 000 **100** 00 **100** **1**/0.13
			1504.2	000 000 **100** 00 **100** **1**/1 000 000 **100** 00 **010** **1**/0.14
1434 ± 2	$2\nu_3 + \nu_4$	1434.9	1436.2	000 **001** 000 00 **200** 0/1 000 **001** 000 00 **110** 0/0.55 000 **001** 000 00 **020** 0/0.52
			1437.7	000 **001** 000 00 **200** 0/1 000 **001** 000 00 **020** 0/0.64 010 **000** 000 00 **100** 1/0.13
			1432.7	000 **010** 000 00 **002** 0/1 000 **010** 000 00 **020** 0/0.63 000 **010** 000 00 **110** 0/0.19
			1434.7	000 **010** 000 00 **200** 0/1 000 **010** 000 00 **002** 0/0.54 000 **001** 000 00 **200** 0/0.4
			1434.4	000 **100** 000 00 **200** 0/1 000 **010** 000 00 **101** 0/0.43 000 **100** 000 00 **020** 0/0.26
1386 ± 2	$2\nu_3 + \nu_6$	1390.1	1385.3	**001** 000 000 00 **002** 0/1 **001** 000 000 00 **011** 0/0.36 001 **000** 000 00 **110** 0/0.2
			1388.0	**001** 000 000 00 **020** 0/1 **001** 000 000 00 **011** 0/0.64 001 **000** 000 00 **110** 0/0.29

DOI: 10.1021/acs.jpca.5b07627
J. Phys. Chem. A 2015, 119, 9557−9567

Table 3. continued

exp	assignment	harm	anharm	character
				IR
			1387.2	**001** 000 000 00 **200** 0/1 **001** 000 000 00 **020** 0/0.46 **001** 000 000 00 **110** 0/0.35
			1394.0	**010** 000 000 00 **020** 0/1 **010** 000 000 00 **200** 0/0.31 **010** 000 000 00 **002** 0/0.22
			1392.1	**010** 000 000 00 **200** 0/1 **010** 000 000 00 **110** 0/0.88 **010** 000 000 00 **011** 0/0.49
			1389.6	**100** 000 000 00 **002** 0/1 **100** 000 000 00 **020** 0/0.27 **100** 000 000 00 **200** 0/0.22
			1391.7	**100** 000 000 00 **200** 0/1 **010** 000 000 00 **110** 0/0.39 **010** 000 000 00 **011** 0/0.29
1386 ± 2	$\nu_1 + \nu_2 + \nu_4$	1397.0	1391.3	000 **001** 000 **01** 000 **1**/1 000 **001** 000 **10** 000 **1**/0.18
			1389.9	000 **001** 000 **10** 000 **1**/1 000 **001** 000 **01** 000 **1**/0.15
			1388.7	000 **010** 000 **01** 000 **1**/1 000 **010** 000 **10** 000 **1**/0.25 000 **100** 000 **01** 000 **1**/0.25
			1387.5	000 **010** 000 **10** 000 **1**/1 000 **100** 000 **10** 000 **1**/0.43 000 **100** 000 **01** 000 **1**/0.39
			1388.0	000 **100** 000 **01** 000 **1**/1 000 **010** 000 **10** 000 **1**/0.46 000 **100** 000 **10** 000 **1**/0.33
			1386.8	000 **100** 000 **10** 000 **1**/1 100 **000** 000 **00** 011 **0**/0.3 000 **010** 000 **10** 000 **1**/0.24
1341, 1335	$\nu_1 + \nu_2 + \nu_6$	1352.1	1346.4	**001** 000 000 **01** 000 **1**/1 **001** 000 000 **10** 000 **1**/0.41 **100** 000 000 **10** 000 **1**/0.15
			1345.4	**001** 000 000 **10** 000 **1**/1 **000** 001 000 **01** 100 **0**/0.95 **000** 001 000 **10** 100 **0**/0.12
			1349.3	**010** 000 000 **01** 000 **1**/1 **010** 000 000 **10** 000 **1**/0.19
			1348.3	**010** 000 000 **10** 000 **1**/1 **100** 000 000 **01** 000 **1**/0.54 **100** 000 000 **10** 000 **1**/0.11
			1348.3	**100** 000 000 **01** 000 **1**/1 **010** 000 000 **10** 000 **1**/0.76 **010** 000 000 **01** 000 **1**/0.18
			1347.0	**100** 000 000 **10** 000 **1**/1 **100** 000 000 **01** 000 **1**/0.14
1290.9 ± 0.5	$\nu_1 + \nu_3$	1304.7	1303.6	000 000 000 00 **001** **1**/1
			1307.0	000 000 000 00 **010** **1**/1
			1306.5	000 000 000 00 **100** **1**/1
1211 ± 2	$2\nu_2 + \nu_6$	1213.1	1199.8	**001** 000 000 **02** 000 0/1 **001** 000 000 **20** 000 0/0.95
			1202.2	**001** 000 000 **02** 000 0/1 **001** 000 000 **20** 000 0/0.54 001 000 000 110 000/0.16
			1204.3	**010** 000 000 **02** 000 0/0.9 **010** 000 000 **20** 000 0/0.89
			1203.7	**100** 000 000 **20** 000 0/0.78 **100** 000 000 **02** 000 0/0.56
1156.9 ± 0.5	$\nu_2 + \nu_3$	1165.7	1159.8	000 000 000 **01** **001** 0/1 000 000 000 **10** **001** 0/0.36
			1163.2	000 000 000 **01** **010** 0/1 000 000 000 **10** **010** 0/0.29
			1163.6	000 000 000 **01** **100** 0/1 000 000 000 **10** **100** 0/0.37 000 000 000 03 0000/0.11
			1157.9	000 000 000 **10** **001** 0/1 000 000 000 **01** **001** 0/0.35
			1160.1	000 000 000 **10** **010** 0/1 000 000 000 **01** **010** 0/0.54
			1159.6	000 000 000 **10** **100** 0/1 000 000 000 **01** **100** 0/0.12
1054 ± 3	$\nu_1 + \nu_4 + \nu_5$	1057.0	1057.5	000 **001** **001** 00 000 **1**/1 000 **001** **010** 00 000 **1**/0.21
			1061.3	000 **001** **010** 00 000 **1**/1 000 **001** **001** 00 000 **1**/0.17
			1055.5	000 **001** **100** 00 000 **1**/1
			1057.1	000 **010** **001** 00 000 **1**/1 000 **010** **010** 00 000 **1**/0.26
			1058.8	000 **010** **010** 00 000 **1**/1 000 **010** **001** 00 000 **1**/1/0.19
			1054.9	000 **010** **100** 00 000 **1**/1 000 **100** **100** 00 000 **1**/1/0.14
			1056.0	000 **100** **001** 00 000 **1**/1 000 **100** **010** 00 000 **1**/0.15
			1057.8	000 **100** **010** 00 000 **1**/1
			1054.1	000 **100** **100** 00 000 **1**/1 000 **010** **100** 00 000 **1**/1/0.14
922 ± 2	$\nu_2 + \nu_4 + \nu_5$	918.03	919.1	000 **001** **001** **01** 000 0/1 000 **001** **010** **01** 000 0/0.18 000 **001** **001** **10** 000 0/0.1
			915.7	000 **001** **001** **10** 000 0/1 000 **001** **010** **10** 000 0/1/0.22
			936.5	000 **001** **010** **01** 000 0/1 000 **001** **001** **01** 000 0/0.17 010 001 000 000 010/0.14
			920.7	000 **001** **010** **10** 000 0/1 000 **001** **100** **01** 000 0/0.67 000 **001** **001** **10**000 0/0.18
			920.9	000 **001** **100** **01** 000 0/1 000 **001** **010** **10** 000 0/0.65 000 **001** **001** **10**000 0/0.12
			914.6	000 **001** **100** **10** 000 0/1
			915.2	000 **010** **001** **01** 000 0/1 000 **100** **001** **01** 000 0/0.22 000 **010** **001** **10**000 0/0.19
			913.9	000 **010** **001** **10** 000 0/1 000 **100** **100** **10** 000 0/0.72 000 **010** **010** **10**000 0/0.29
			934.6	000 **010** **010** **01** 000 0/1 000 **010** **001** **01** 000 0/0.17
			915.1	000 **010** **010** **10** 000 0/1 000 **100** **001** **01** 000 0/0.22 000 **010** **001** **10**000 0/0.14
			916.8	000 **010** **100** **01** 000 0/1 000 **100** **100** **01** 000 0/0.29 000 **010** **100** **10**000 0/0.11
			912.6	000 **010** **100** **10** 000 0/1
			914.8	000 **100** **001** **10** 000 0/0.78 000 **100** **00101**0000/0.58 000 **10001010**0000/0.16
			932.7	000 **100** **010** **01** 000 0/1 000 000 110 01 000 0/0.48 000 **100** **001** **01**000 0/0.16
			916.1	000 **100** **010** **10** 000 0/1 000 **100** **001** **01** 000 0/0.12
			916.5	000 **100** **100** **01** 000 0/1 000 **010** **100** **01** 000 0/0.29 000 **100** **100** **10**000 0/0.12
			913.8	000 **100** **100** **10** 000 0/1 000 **010** **001** **10** 000 0/0.92 000 **010** **010** **10**000 0/0.24
905 ± 2	$\nu_3 + 2\nu_6$	898.8	891.6	**002** 000 000 00 **001** 0/1 101 000 000 000010/0.21 **200** 000 000 00 **001** 0/0.19
			893.8	**002** 000 000 00 **100** 0/1 **200** 000 000 00 **100** 0/0.19 101 000 000 001 000/0.15
			904.1	**020** 000 000 00 **010** 0/1 011 000 000 000 100/0.28 110 000 000 000 100/0.18
			899.0	**200** 000 000 00 **001** 0/1 110 000 000 000 010/0.38 011 000 000 000 100/0.37

DOI: 10.1021/acs.jpca.5b07627
J. Phys. Chem. A 2015, 119, 9557−9567

Table 3. continued

exp	assignment	harm	anharm	character
				IR
			900.3	**020** 000 000 00 **001** 0/0.99 **200** 000 000 00 **001** 0/1 011 000 000 000 010/0.82
			901.6	**200** 000 000 00 **100** 0/1 011 000 000 000 010/0.28 **200** 000 000 00 **001** 0/0.21
852.8 ± 0.5	$\nu_1 + \nu_4$	858.3	857.8	000 **001** 000 00 000 **1**/1
			854.1	000 **010** 000 00 000 **1**/1
			854.5	000 **100** 000 00 000 **1**/1
827, 821	$\nu_3 + \nu_5$	825.8	824.2	000 000 **001** 00 **001** 0/1 000 000 **100** 00 **001** 0/0.46 000 000 **010** 00**001** 0/0.16
			826.3	000 000 **001** 00 **010** 0/1 000 000 **100** 00 **010** 0/0.45 000 000 **010** 00**010** 0/0.12
			826.9	000 000 **001** 00 **100** 0/1 000 000 **100** 00 **100** 0/0.48 000 000 **010** 00**100** 0/0.14
			826.0	000 000 **010** 00 **001** 0/1 000 000 **100** 00 **001** 0/0.1
			827.6	000 000 **001** 00 **010** 0/1 000 000 **100** 00 **010** 0/0.12
			828.5	000 000 **001** 00 **100** 0/1 000 000 **100** 00 **100** 0/0.13
			821.7	000 000 **100** 00 **001** 0/1 000 000 **001** 00 **001** 0/0.37 000 000 **010** 00**001** 0/0.15
			823.7	000 000 **100** 00 **010** 0/1 000 000 **001** 00 **010** 0/0.36 000 000 **010** 00**010** 0/0.14
			824.4	000 000 **100** 00 **100** 0/1 000 000 **001** 00 **100** 0/0.39 000 000 **010** 00**100** 0/0.17
719.1 ± 0.5	$\nu_2 + \nu_4$	719.3	713.6	000 **001** 000 **01** 000 0/1 000 **001** 000 **10** 000 0/0.19
			711.1	000 **001** 000 **10** 000 0/1
			711.4	000 **010** 000 **01** 000 0/1 000 **010** 000 **10** 000 0/0.17
			708.8	000 **010** 000 **10** 000 0/1
			710.6	000 **100** 000 **01** 000 0/1 000 **100** 000 **10** 000 0/0.13
			708.5	000 **100** 000 **10** 000 0/1
677.5, 670	$\nu_2 + \nu_6$	674.5	668.5	**001** 000 000 **01** 000 0/1 **001** 000 000 **10** 000 0/0.17
			666.3	**001** 000 000 **10** 000 0/1
			671.2	**010** 000 000 **01** 000 0/1 **010** 000 000 **10** 000 0/0.18
			668.7	**010** 000 000 **10** 000 0/1
			669.9	**100** 000 000 **01** 000 0/1 **100** 000 000 **10** 000 0/0.16
			667.7	**100** 000 000 **10** 000 0/1
585 ± 5	$\nu_4 + 2\nu_5$	578.1	582.3	000 **001 002** 00 000 0/1 000 **001 020** 00 000 0/0.61 000 **001 200** 00 0000/0.61
			585.3	000 **001 020** 00 000 0/1 000 **001 101** 00 000 0/0.63 000 **001 110** 00 0000/0.53
			581.4	000 **010 002** 00 000 0/1 000 **010 200** 00 000 0/0.8 000 **010 020** 00 000 0/0.62
			583.6	000 **010 020** 00 000 0/1 000 **010 101** 00 000 0/0.78 000 **010 110** 00 0000/0.75
			582.8	000 **100 020** 00 000 0/1 000 **100 101** 00 000 0/0.79 000 **100 002** 00 000 0/0.6
546 ± 2	$3\nu_4$	542.2	540.7	000 **003** 000 00 000 0/1.6 000 **021** 000 00 0000/1.2 000 **201** 000 00 0000/0.51
			533.7	000 **030** 000 00 000 0/1 010 000 110 00 000 0/0.53 000 **210** 000 00 000 0/0.5
519.5 ± 2	$2\nu_4 + \nu_6$	497.3	498.4	**001 002** 000 00 000 0/1 **001 200** 000 00 000 0/0.35 **001 110** 000 00 0000/0.28
			491.9	**001 020** 000 00 000 0/1 **001 200** 000 00 000 0/0.56 **001 002** 000 00 0000/0.34
			496.0	**001 200** 000 00 000 0/1 **001 020** 000 00 000 0/0.34 **010 011** 000 00 0000/0.21
			502.8	**010 002** 000 00 000 0/1 **010 020** 000 00 000 0/0.8 **100 002** 000 00 000 0/0.35
			495.0	**010 020** 000 00 000 0/1 **010 200** 000 00 000 0/0.63 **010 002** 000 00 0000/0.36
			501.6	**100 002** 000 00 000 0/1 **001 010** 000 00 000 0/0.66 **010 020** 000 00 0000/0.62
			496.3	**100 020** 000 00 000 0/1 **001 200** 000 00 000 0/0.12 **010 020** 000 00 000 0/0.1
			498.1	**100 200** 000 00 000 0/1 **100 002** 000 00 000 0/0.47 **001 002** 000 00 0000/0.29
419 ± 2	$3\nu_6$	407.6	399.0	**003** 000 000 00 000 0/1 **021** 000 000 00 000 0/0.19 **201** 000 000 00 0000/0.17
			409.2	**300** 000 000 00 000 0/1 **102** 000 000 00 000 0/0.23 **120** 000 000 00 0000/0.19
337.2 ± 2	$\nu_5 + \nu_6$	334.5	335.9	**001** 000 **001** 00 000 0/1 **001** 000 **100** 00 000 0/0.38 **001** 000 **010** 00 0000/0.16
			338.0	**001** 000 **010** 00 000 0/1 **001** 000 **001** 00 000 0/0.11
			333.3	**001** 000 **100** 00 000 0/1 **001** 000 **001** 00 000 0/0.33
			339.0	**010** 000 **001** 00 000 0/1 **010** 000 **100** 00 000 0/0.38 **100** 000 **010** 00 0000/0.38
			336.3	**010** 000 **100** 00 000 0/1 **010** 000 **001** 00 000 0/0.31 **010** 000 **010** 00 0000/0.25
			336.8	**100** 000 **001** 00 000 0/1 **100** 000 **100** 00 000 0/0.57 **001** 000 **001** 00 0000/0.12
			339.1	**100** 000 **010** 00 000 0/1 **010** 000 **001** 00 000 0/0.83 **010** 000 **010** 00 0000/0.82
			339.3	**100** 000 **010** 00 000 0/1 **010** 000 **010** 00 000 0/0.33 **010** 000 **001** 000000/0.28
			334.9	**100** 000 **100** 00 000 0/1 **100** 000 **001** 00 000 0/0.46

[a]Leading basis functions (with relative amplitudes above 0.1) used to assign the transitions and their relative amplitudes (after "/") are also given. The basis function character is given by a list of $n(i,d)$, d = 1, ..., 15. In bold are highlighted normal modes where excitations (non-zero n values) are expected on the basis of the experimental assignments.

experimental and computational results.[8,10,54−58] We note that only the f_1u modes are IR active. When a harmonic PES is used, the rectangular collocation approach reproduces both the transitions and the splittings to within 0.2 cm^{-1}. This is true regardless of whether both the basis and the energies are fit with eqs 10 and 11 or whether only the basis is fit with eqs 10 and 11 and the squared collocation eigenproblem, eq 12, is used to determine the energies. This demonstrates the accuracy of the

DOI: 10.1021/acs.jpca.5b07627
J. Phys. Chem. A 2015, 119, 9557−9567

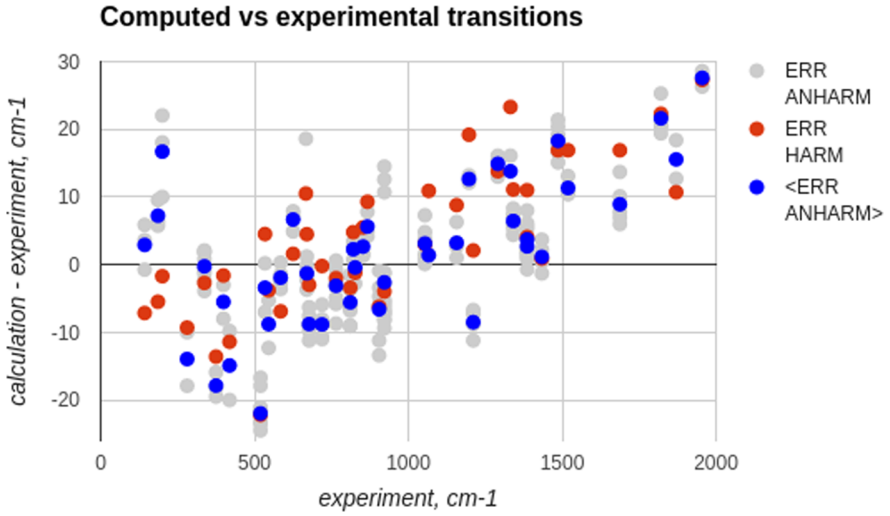

Figure 2. Difference between the computed and experimental transitions in UF_6, in the harmonic (ERR HARM, red dots) and anharmonic (ERR ANHARM, gray dots) approximation. For the anharmonic approximation, the average errors over the transitions with the same character are also shown (<ERR ANHARM>, blue dots).

method. The method does not impose symmetry; therefore, all 15 mode frequencies are listed, showing that splittings between levels that, by symmetry, should be exactly degenerate are very small (these splittings can be compared to differences among harmonic levels that should be degenerate but are as large as 1 cm^{-1} in Gaussian 09 if no symmetry is imposed).

A plot of DFT energies against harmonic potential energies, both evaluated at all of the 50 000 points, is shown in Figure 1. The scatter or width implies that points with similar harmonic potential energies have rather different DFT energies. This demonstrates that anharmonicity/coupling is noticeable although relatively weak. The (harmonic) ZPE is about 2595 cm^{-1}. Transitions with respect to the ZPE up to 1955 cm^{-1} are reported in this paper and are significantly affected by anharmonicity and coupling. With the right choice of the parameters, the basis functions we use are exact eigenfunctions of the harmonic Hamiltonian and therefore one expects the fit to be poorer when the anharmonicity and coupling are larger. The fact that $R \sim 5 \times 10^{-3}$ for the anharmonic calculation (much larger than for the harmonic calculation where $R \sim 2 \times 10^{-5}$) is thus also demonstration of the importance of anharmonicity/coupling. Using the fitted basis, 816 levels were computed with eq 12. In spite of the extremely small number of *ab initio* points, the spectrum is converged with respect to the number of points: a data set with 30 000 points results in changes in most levels by less than 0.1 cm^{-1}; out of 816 levels, 4 levels differ by about 0.3 cm^{-1} and 38 levels by about 0.2 cm^{-1}.

Tables 2 and 3 list vibrational levels that have been measured (either with Raman or with IR spectroscopy) and previously assigned.[5] We assigned computed levels by using the basis functions with the largest amplitudes. These are also listed in Tables 2 and 3. For example, the level with the largest coefficient for the basis function having two quanta in mode 15 is designated as 000 000 000 00 000 **2** (i.e., the 15 $n(i,d)$ are listed in the order d = 1, ..., 15; see eq 8). It is assigned to the measured (Raman) transition at 1331.9 ± 1 cm^{-1}, which was assigned as $2\nu_1$,[5] and so on. Tables 2 and 3 list the three most important basis functions and their relative amplitudes after "/". The corresponding harmonic wavenumbers (from collocation calculations) are also given. In Tables 2 and 3 one sees that whereas the assignments for the fundamentals are unambiguous, for many other levels several basis functions are important. This demonstrates that coupling is important. In general, one harmonic level corresponds to a cluster of anharmonic levels. Degeneracy of harmonic levels is lifted by coupling. For example, the measured (Raman) transition at 399 ± 2 cm^{-1} corresponds to two computed transitions, whereas in both cases the largest coefficient is for one of the degenerate basis functions with $2\nu_5$ character, 000 000 **200** 00 000 0 and 000 000 **020** 00 000 0, respectively, the first one at 391.0 cm^{-1} has also contributions from 000 000 **110** 00 000 0 and 000 000 **002** 00 000 0 and the second one from 000 000 **110** 00 000 0 and 000 000 **101** 00 000 0. Overall, anharmonicity and coupling induce changes in levels and transitions on the order of 10 cm^{-1}; i.e., the effect is mild yet noticeable. Table 2 also shows that although the isotopologue splittings of the ν_3 and ν_4 modes are similar in the harmonic and anharmonic approximations, within the accuracy of the method, the isotopologue splittings of the ν_2 and ν_5 modes are not. The isotopologue splittings of the ν_2 and ν_5 modes are significant in the anharmonic calculation and not in the harmonic calculation. This would be expected if the ν_2 and ν_5 modes were significantly affected by coupling, but although the transition at 534.3 cm^{-1} is clearly influenced by coupling, the other ν_2 and ν_5 transitions are not (i.e., the contributing basis functions all have ν_2 and ν_5 character, respectively). The magnitude of splitting of these modes for which coupling does not seem important (up to 0.5 cm^{-1}) might therefore be indicative of the accuracy of the solution of the Schrödinger equation.

Figure 2 shows the differences between the computed and experimentally assigned transitions calculated from the harmonic and anharmonic levels. In the anharmonic case, we also show the average error for transitions with the same (leading) character. We note that experimental UF_6 spectra have broad peaks with widths of dozens cm^{-1},[1,8] for which the peak maximum is reported. The average energy for levels with the same character is thus comparable to the position of an experimental peak. Both types of calculations differ from the experimental transitions by about 10 cm^{-1}. This comparison is, however, not indicative of the accuracy of the method, as it subsumes errors due to the DFT calculations. This work aims to compute an anharmonic spectrum from *ab initio* data of a given level of theory. The anharmonic calculation does improve the quality of the spectrum. One indication

DOI: 10.1021/acs.jpca.5b07627
J. Phys. Chem. A 2015, 119, 9557−9567

of this is that the use of the tuned basis lowers the ZPE vs the harmonic basis by 4.7 cm^{-1} and lowers the energy of most levels (even as energies of some transitions increase because the ZPE is lowered by more than the corresponding level). Another indication is the fact that the anharmonic calculation is able to reproduce qualitative features that are not reproducible in principle with the harmonic approximation. For example, two measured transitions, at 821 and 827 cm^{-1}, were assigned as $\nu_3 + \nu_5$.[5] The anharmonic calculation has two clusters of wavenumbers with this character, one ranging 821.7−824.4 cm^{-1} and one ranging 826.3−828.5 cm^{-1}, whereas the harmonic calculation necessarily results in a single transition at 825.8 cm^{-1}. Another example is the experimental peak at 1386 ± 2 cm^{-1}, which was assigned to overlapping excitations with character $2\nu_3 + \nu_6$ and $\nu_1 + \nu_2 + \nu_4$. The harmonic calculation positions these transitions at 1390.1 and 1397.0 cm^{-1}, i.e., well-separated, whereas the anharmonic calculation results in clusters of wavenumbers ranging 1385.3−1394.0 and 1386.8−1391.2 cm^{-1}, with average values of 1389.7 and 1388.7 cm^{-1}, respectively, i.e., overlapping in agreement with the experimental data.

CONCLUSIONS

The anharmonic spectrum of UF_6 has been computed, for the first time, without neglecting anharmonicity and coupling, in a 15-dimensional configuration space. The spectrum is computed directly from a relatively small number of *ab initio* points, bypassing the construction of a PES. We used 50 000 *ab initio* energies. If the points had been on a direct product grid, the density of sampling would have been only about 2.1 data per DOF. The 50 000 points nevertheless converge most levels to better than 0.1 cm^{-1}. To solve the vibrational Schrödinger equation, a rectangular (i.e., with more potential points than basis functions) collocation approach was used, in which the basis set is adapted via parametrization. It is the flexible nature of the basis and consequently its small size that permit using such a small number of potential points that they are computable directly *ab initio*.

In the energy range up to about 5000 cm^{-1} above the potential minimum (relevant to the computation of the assigned transitions), the difference between the normal mode based harmonic PES and the *ab initio* PES is perceptible, reaching about ±1000 cm^{-1} at the top of the range. However, the computed anharmonic spectrum differs from the harmonic spectrum by only several cm^{-1} for most transitions. This difference is still significant as it would, e.g., affect the tuning of the laser used for isotopologue-selective detection or excitation. Both the anharmonic and the harmonic spectra differ from the experimental transitions by about 10 cm^{-1}. This comparison is, however, not directly indicative of the effect of anharmonicity and coupling, as it subsumes the error due to the DFT calculations. The anharmonic calculation with the fitted basis does improve the quality of the spectrum, as evidenced by the lowering of the ZPE and of most levels achieved by fitting the basis parameters, as well as by reproducing some qualitative features of the spectrum that cannot be obtained in the harmonic approximation.

AUTHOR INFORMATION

Corresponding Author

*S. Manzhos. E-mail: mpemanzh@nus.edu.sg. Fax: +65 6779 1459.

Author Contributions

The manuscript was written through contributions of all authors. All authors have given approval to the final version of the manuscript.

Funding

This work was supported by AcRF grants from The Ministry of Education of Singapore (SM) and by the National Science and Engineering Research Council of Canada (TC and NM).

Notes

The authors declare no competing financial interest.

ABBREVIATIONS

PES, potential energy surface; DFT, density functional theory; IR, infrared; ECP, effective core potential; DOF, degree of freedom; LHS, left-hand side; RHS, right-hand side; KEO, kinetic energy operator

REFERENCES

(1) Berezin, A. G.; Malyugin, S. L.; Nadezhdinskii, A. I.; Namestnikov, D. Y.; Ponurovskii, Y. Y.; Stavrovskii, D. B.; Shapovalov, Y. P.; Vyazov, I. E.; Zaslavskii, V. Y.; Selivanov, Y. G.; et al. UF_6 Enrichment Measurements Using TDLS Techniques. *Spectrochim. Acta, Part A* **2007**, *66*, 796−802.

(2) Koh, Y. W.; Westerman, K.; Manzhos, S. A Computational Study of Adsorption and Vibrations of UF_6 on Graphene Derivatives: Conditions for 2D Enrichment. *Carbon* **2015**, *81*, 800−806.

(3) USNRC Technical Training Center. Module 3.0: Laser Enrichment Methods (AVLIS and MLIS), http://pbadupws.nrc.gov/docs/ML1204/ML12045A051.pdf; 2008; pp 2−7.

(4) Wolfsberg, M.; Van Hook, W. A.; Paneth, P. Isotope Separation. In *Isotope Effects*; Springer: The Netherlands, 2009; pp 264−266.

(5) Schneider, E.; Carlsen, B.; Tavrides, E.; van der Hoeven, C.; Phathanapirom, U. Measures of the Environmental Footprint of the Front End of the Nuclear Fuel Cycle. *Energy Econ.* **2013**, *40*, 898−910.

(6) Parvin, P.; Sajad, B.; Silakhori, K.; Hooshvar, M.; Zamanipour, Z. Molecular Laser Isotope Separation Versus Atomic Vapor Laser Isotope Separation. *Prog. Nucl. Energy* **2004**, *44*, 331−45.

(7) Ronander, E.; Strydom, H. J.; Botha, L. R. High-Pressure Continuously Tunable CO_2 Lasers and Molecular Laser Isotope Separation. *Pramana* **2014**, *82*, 49−58.

(8) McDowell, R. S.; Asprey, L. B.; Paine, R. T. Vibrational Spectrum and Force Field of Uranium Hexafluoride. *J. Chem. Phys.* **1974**, *61*, 3571−3580.

(9) Zhang, Y. G.; Zha, X. W. Calculations of the Vibrational Frequency and Isotopic Shift of UF_6 and U_2F_6. *Chin. Phys. B* **2012**, *21*, 073301.

(10) Odoh, S. O.; Schrekenbach, G. Performance of Relativistic Effective Core Potentials in DFT Calculations on Actinide Compounds. *J. Phys. Chem. A* **2010**, *114*, 1957−1963.

(11) Papoušek, D.; Aliev, M. R. Molecular Vibrational and Rotational Spectra. *Studies in Physical and Theoretical Chemistry*; Elsevier Scientific Publishing Company: Amsterdam, 1982; p 17.

(12) Bowman, J. M. Self-Consistent Field Energies and Wavefunctions for Coupled Oscillators. *J. Chem. Phys.* **1978**, *68*, 608−10.

(13) Roy, T. K.; Gerber, R. B. Vibrational Self-Consistent Field Calculations for Spectroscopy of Biological Molecules: New Algorithmic Developments and Applications. *Phys. Chem. Chem. Phys.* **2013**, *15*, 9468−92.

(14) Carter, S.; Handy, N. C. The Variational Method for the Calculation of Ro-vibrational Energy Levels. *Comput. Phys. Rep.* **1986**, *5*, 117−171.

(15) Sibert, E. L. Variational and Perturbative Descriptions of Highly Vibrationally Excited Molecules. *Int. Rev. Phys. Chem.* **1990**, *9*, 1−27.

(16) Tennyson, J. The Calculation of the Vibration-Rotation Energies of Triatomic Molecules Using Scattering Coordinates. *Comput. Phys. Rep.* **1986**, *4*, 1−36.

(17) Yang, W. T.; Peet, A. C. The Collocation Method for Bound Solutions of the Schrodinger Equation. *Chem. Phys. Lett.* **1988**, *153*, 98−104.

(18) Peet, A. C.; Yang, W. T. The Collocation Method for Calculating Vibrational Bound States of Molecular Systems − with Application to Ar-HCl. *J. Chem. Phys.* **1989**, *90*, 1746−1751.

DOI: 10.1021/acs.jpca.5b07627
J. Phys. Chem. A 2015, 119, 9557−9567

(19) Yang, W.; Peet, A. C. A Method for Calculating Vibrational Bound States − Iterative Solution of the Collocation Equations Constructed from Localized Basis Sets. *J. Chem. Phys.* **1990**, *92*, 522−6.
(20) Avila, G.; Carrington, T. Solving the Schroedinger Equation Using Smolyak Interpolants. *J. Chem. Phys.* **2013**, *139*, 134114.
(21) Bowman, J. M.; Carrington, T.; Meyer, H. D. Variational Quantum Approaches for Computing Vibrational Energies of Polyatomic Molecules. *Mol. Phys.* **2008**, *106*, 2145−82.
(22) Boys, S. F. Some Bilinear Convergence Characteristics of Solutions of Dissymmetric Secular Equations. *Proc. R. Soc. London, Ser. A* **1969**, *309*, 195−208.
(23) Poirier, B. Using Wavelets to Extend Quantum Dynamics Calculations to Ten or More Degrees of Freedom. *J. Theor. Comput. Chem.* **2003**, *2*, 65−72.
(24) Shimshovitz, A.; Tannor, D. J. Phase-Space Approach to Solving the Time-Independent Schrodinger Equation. *Phys. Rev. Lett.* **2012**, *109*, 070402.
(25) Brown, J.; Carrington, T., Jr Using an Iterative Eigensolver to Compute Vibrational Energies with Phase-Spaced Localized Basis Functions. *J. Chem. Phys.* **2015**, *143*, 044104.
(26) Bačić, Z.; Light, J. C. Theoretical Methods for Rovibrational States of Floppy Molecules. *Annu. Rev. Phys. Chem.* **1989**, *40*, 469−98.
(27) Henderson, J. R.; Tennyson, J. All the Vibrational Bound States of H_3^+. *Chem. Phys. Lett.* **1990**, *173*, 133−8.
(28) Bramley, M. J.; Handy, N. C. Efficient Calculation of Rovibrational Eigenstates of Sequentially Bonded 4-Atom Molecules. *J. Chem. Phys.* **1993**, *98*, 1378−97.
(29) Wang, X. G.; Carrington, T., Jr. New Ideas for Using Contracted Basis Functions with a Lanczos Eigensolver for Computing Vibrational Spectra of Molecules with Four or More Atoms. *J. Chem. Phys.* **2002**, *117*, 6923−34.
(30) Yu, H. G. Two-Layer Lanczos Iteration Approach to Molecular Spectroscopic Calculation. *J. Chem. Phys.* **2002**, *117*, 8190−6.
(31) Chan, M.; Carrington, T.; Manzhos, S. Anharmonic Vibrations of the Carboxyl Group in Acetic Acid on TiO_2: Implications for Adsorption Mode Assignment in Dye-Sensitized Solar Cells. *Phys. Chem. Chem. Phys.* **2013**, *15*, 10028−10034.
(32) Manzhos, S.; Chan, M.; Carrington, T. Communication: Favourable Dimensionality Scaling of Rectangular Collocation with Adaptable Basis Functions up to 7 Dimensions. *J. Chem. Phys.* **2013**, *139*, 051101.
(33) Boutry, G.; Elad, M.; Golub, G. H.; Milanfar, P. The Generalized Eigenvalue Problem for Nonsquare Pencils Using a Minimal Perturbation Approach. *SIAM J. Matrix Anal. Appl.* **2005**, *27*, 582−601.
(34) Manzhos, S.; Yamashita, K.; Carrington, T. On the Advantages of a Rectangular Matrix Collocation Equation for Computing Vibrational Spectra from Small Basis Sets. *Chem. Phys. Lett.* **2011**, *511*, 434−439.
(35) Braams, B. J.; Bowman, J. M. Permutationally Invariant Potential Energy Surfaces in High Dimensionality. *Int. Rev. Phys. Chem.* **2009**, *28*, 577−606.
(36) Dawes, R.; Thompson, D. L.; Wagner, A. F.; Minkoff, M. Interpolating Moving Least-Squares Methods for Fitting Potential Energy Surfaces: a Strategy for Efficient Automatic Data Point Placement in High Dimensions. *J. Chem. Phys.* **2008**, *128*, 084107.
(37) Manzhos, S.; Carrington, T. Using Redundant Coordinates to Represent Potential Energy Surfaces with Lower-Dimensional Functions. *J. Chem. Phys.* **2007**, *127*, 014103.
(38) Anselmi, C.; Mosconi, E.; Pastore, M.; Ronca, E.; De Angelis, F. Adsorption of Organic Dyes on TiO_2 Surfaces in Dye-Sensitized Solar Cells: Interplay of Theory and Experiment. *Phys. Chem. Chem. Phys.* **2012**, *14*, 15963−74.
(39) Christensen, P. A.; Jones, S. W. M.; Hamnett, A. In Situ FTIR Studies of Ethanol Oxidation at Polycrystalline Pt in Alkaline Solution. *J. Phys. Chem. C* **2012**, *116*, 24681−9.
(40) Li, D. L.; Sakai, S.; Nakagawa, Y.; Tomishige, K. FTIR Study of CO Adsorption on Rh/MgO Modified with Co, Ni, Fe or CeO_2 for the Catalytic Partial Oxidation of Methane. *Phys. Chem. Chem. Phys.* **2012**, *14*, 9204−13.
(41) Manzhos, S.; Yamashita, K.; Carrington, T. Using a Neural Network Based Method to Solve the Vibrational Schrödinger Equation for H_2O. *Chem. Phys. Lett.* **2009**, *474*, 217−221.
(42) Manzhos, S.; Carrington, T.; Yamashita, K. Calculating Anharmonic Vibrational Frequencies of Molecules Adsorbed on Surfaces Directly from Ab Initio Energies with a Molecule-Independent Method: H_2O on Pt(111). *Surf. Sci.* **2011**, *605*, 616−622.
(43) Chan, M.; Yamashita, K.; Carrington, T.; Manzhos, S. Towards Accurate Spectroscopic Identification of Species at Catalytic Surfaces: Anharmonic Vibrations of Formate on AuPt. *MRS Proc.* **2012**, *1484*, imrc12-1484-71-0016.
(44) Hohenberg, P.; Kohn, W. Inhomogeneous Electron Gas. *Phys. Rev.* **1964**, *136*, B864−71.
(45) Kohn, W.; Sham, L. J. Self-Consistent Equations Including Exchange and Correlation Effects. *Phys. Rev.* **1965**, *140*, A1133−A38.
(46) Perdew, J. P.; Burke, K.; Ernzerhof, M. Generalized Gradient Approximation Made Simple. *Phys. Rev. Lett.* **1996**, *77*, 3865−68.
(47) Perdew, J. P.; Burke, K.; Ernzerhof, M. Errata: Generalized Gradient approximation Made Simple. *Phys. Rev. Lett.* **1997**, *78*, 1396.
(48) Adamo, C.; Barone, V. Toward Reliable Density Functional Methods without Adjustable Parameters: the PBE0Model. *J. Chem. Phys.* **1999**, *110*, 6158−69.
(49) Kuchle, W.; Dolg, M.; Stoll, H.; Preuss, H. Energy-Adjusted Pseudopotentials for the Actinides − Parameter Sets and Test Calculations for Thorium and Thorium Monoxide. *J. Chem. Phys.* **1994**, *100*, 7535−42.
(50) Cao, X. Y.; Dolg, M.; Stoll, H. Valence Basis Sets for Relativistic Energy-Consistent Small-Core Actinide Pseudopotentials. *J. Chem. Phys.* **2003**, *118*, 487−96.
(51) Cao, X. Y.; Dolg, M. Segmented Contraction Scheme for Small-Core Actinide Pseudopotential Basis Sets. *J. Mol. Struct.: THEOCHEM* **2004**, *673*, 203−9.
(52) Schafer, A.; Huber, C.; Ahlrichs, R. Fully Optimized Contracted Gaussian Basis Sets of Triple Zeta Valence Quality for Atoms Li to Kr. *J. Chem. Phys.* **1994**, *100*, 5829−35.
(53) Frisch, M. J.; Trucks, G. W.; Schlegel, H. B.; Scuseria, G. E.; Robb, M. A.; Cheeseman, J. R.; Scalmani, G.; Barone, V.; Mennucci, B.; Petersson, G. A.; et al. *Gaussian 09*, Revision D.01; Gaussian, Inc.: Wallingford, CT, 2009.
(54) Kimura, M.; Schomaker, V.; Smith, D. W.; Weinstock, B. Electron-Diffraction Investigation of the Hexafluorides of Tungsten, Osmium, Iridium, Uranium, Neptunium, and Plutonium. *J. Chem. Phys.* **1968**, *48*, 4001−4011.
(55) Seip, H. M. Studies on the Failure of the First Born Approximation in Electron Diffraction. I. Uranium Hexafluoride. *Acta Chem. Scand.* **1965**, *19*, 1955−1968.
(56) Pantazis, A.; Neese, F. All-Electron Scalar Relativistic Basis Sets for the Actinides. *J. Chem. Theory Comput.* **2011**, *7*, 677−84.
(57) Batista, E. R.; Martin, R. L.; Hay, P. J.; Peralta, J. E.; Scuseria, G. E. Density Functional Investigations of the Properties and Thermochemistry of UF_6 and UF_5 Using Valence-Electron and All-Electron Approaches. *J. Chem. Phys.* **2004**, *121*, 2144−50.
(58) Song, W. Z.; Gu, D. Infrared Absorption Spectrum of Uranium Hexafluoride at Lower Temperature. *J. Nucl. Radiochem.* **1990**, *12*, 175−179.
(59) van Lenthe, E.; Baerends, E. J.; Snijders, J. G. Relativistic Energy Using Regular Approximations. *J. Chem. Phys.* **1994**, *101*, 9783−92.
(60) Weigend, F.; Ahlrichs, R. Balanced Basis Sets of Split Valence, Triple Zeta and Quadruple Zeta Valence Quality for H to Rn: Design and Assessment of Accuracy. *Phys. Chem. Chem. Phys.* **2005**, *7*, 3297−305.
(61) Sobol, I. M. On the Distribution of Points on a Cube and the Approximate Evaluation of Integrals. *USSR Comput. Math. Math. Phys.* **1967**, *7*, 86−112.
(62) Chan, M.; Manzhos, S.; Carrington, T.; Yamashita, K. Parameterized Bases for Calculating Vibrational Spectra Directly from Ab Initio Data Using Rectangular Collocation. *J. Chem. Theory Comput.* **2012**, *8*, 2053−2061.

DOI: 10.1021/acs.jpca.5b07627
J. Phys. Chem. A 2015, 119, 9557−9567

(63) Avila, G.; Carrington, T., Jr. Nonproduct Quadrature Grids for Solving the Vibrational Schrodinger Equation. *J. Chem. Phys.* **2009**, *131* (2009), 174103.
(64) Avila, G.; Carrington, T. Using a Pruned Basis, a Non-Product Quadrature Grid, and the Exact Watson Normal-Coordinate Kinetic Energy Operator to Solve the Vibrational Schrodinger Equation for C_2H_4. *J. Chem. Phys.* **2011**, *135*, 064101.
(65) *Matlab* Release 2014a; The MathWorks, Inc.: Natick, MA, 2014.
(66) Meier, P.; Oschetzki, D.; Berger, R.; Rauhut, G. Transformation of Potential Energy Surfaces for Estimating Isotopic Shifts in Anharmonic Vibrational Frequency Calculations. *J. Chem. Phys.* **2014**, *140*, 184111.

DOI: 10.1021/acs.jpca.5b07627
J. Phys. Chem. A 2015, 119, 9557−9567